Generation of conical and spherical second harmonics in three-dimensional nonlinear photonic crystals with radial symmetry

Junjie Chen and Xianfeng Chen*

Department of Physics, the State Key Laboratory on Fiber Optic Local Area Communication Networks and Advanced Optical Communication Systems, Shanghai, Jiao Tong University, 800 Dongchuan Road, Shanghai 200240, China
**Corresponding author: xfchen@sjtu.edu.cn*

Received September 7, 2010; revised November 12, 2010; accepted November 16, 2010;
posted November 17, 2010 (Doc. ID 134689); published January 10, 2011

Two types of radially symmetric three-dimensional nonlinear photonic crystals with the cylindrical structure and the egglike structure are proposed, from which the conical and the spherical quadratic harmonic waves can be produced, respectively, by three-dimensional quasi-phase matching. First, the cylindrical structures with periodic and aperiodic modulations of the nonlinear coefficient are both studied, showing their significant advantages compared to the corresponding two-dimensional structures. The dependencies of the transverse and the longitudinal phase-matching periods on harmonic propagating directions are also calculated and analyzed. Then, the egglike structure is designed by programming and the distribution of reciprocal vectors is presented, indicating its ability to generate the spherical harmonic as a point light source. The investigation of the intensity distribution on the spherical wavefront is also performed, showing its strong dependence on the harmonic polarization and the quadratic nonlinear coefficients.

OCIS codes: 140.3380, 050.5298.

1. INTRODUCTION

Nonlinear photonic crystals (NPCs) associated with quasi-phase-matching (QPM) technique [1] are created by the modulation of quadratic nonlinear coefficients so as to result in realizing the expected optical parametric process. By extending the one-dimensional (1D) QPM theory into the two-dimensional (2D) one, the 2D NPC was first proposed by Berger in 1998 [2]. Ever since then, plenty of work has been comprehensively done on the 2D NPC, of which some popular issues are, for example, the nonlinear Cerenkov radiation in 2D NPCs [3–6], the broadband frequency doubling in random phase-matching media [7–13], and the nonlinear Bragg diffraction in annular periodically poled NPCs [14–18]. These novel phenomena which cannot be observed in 1D structures deeply reveal lots of new physical origins, substantially enlarging the research scope of QPM.

Recently, the NPC has been further generalized into the three-dimensional (3D) case [19] by us, which may provide more abundant reciprocal lattice vectors (RLVs) with additional spatial freedom to compensate the phase mismatches in the optical parametric processes that cannot occur in the 1D or 2D regime, making the RV design more flexible. Although the fabrication of 3D NPCs is extremely difficult, many experimental explorations have been done. The most possible realization of the 3D NPC now seems to be the domain reversal induced by ultraviolet pulses [20,21] and femtosecond laser [22–24] due to the relatively convenient operation of light which avoids the complicated scheme including multiple steps such as bonding, cutting, and regrowth. Once the fabrication of the 3D NPC comes true, a great deal of work may be concentrated on this newly arisen research direction. Consequently, the theoretical design and study of new structures appear to be very necessary for the practical application of 3D NPCs.

In this paper, we design to our knowledge, two novel radially symmetric structures, namely, the cylindrical structure and the egglike structure for the 3D NPC. The former is derived by adding an additional longitudinal modulation to the conventional 2D annular structure such that the generated conical harmonic wave may have an arbitrary apex angle in contrast to the fixed one in a 2D structure. The latter is created via programming so that the spherical second harmonic may be emitted from the egglike structure which can be considered a point light source. The unique properties of these two structures are also analyzed for further understanding.

2. CYLINDRICAL STRUCTURE

The design of the cylindrical structure is enlightened by the traditional 2D annular NPC as shown in Fig. 1(a) which exhibits radial symmetry (rotational symmetry along the poling direction, namely, the z axis) and possesses an infinite number of RLVs arranged in the crystal plane, namely, the x-y plane. Saltiel *et al.* [14,15,17] have deeply studied this kind of structure by irradiating the fundamental beam along the z axis. The conical second harmonic may result from it via the nonlinear Bragg diffraction since the phase-matching condition is $2\vec{k}_\omega + \vec{G}_{t'} = \vec{k}_{2\omega}$, where $\vec{k}_\omega$ is the fundamental wave vector, $\vec{k}_{2\omega}$ is the harmonic wave vector, and the transverse phase mismatch is compensated by the RLV $\vec{G}_{t'}$ [see Fig. 1(b)]. However, as it can be seen, the vertex angle $2\theta'$ is a fixed value of $\arccos(2k_\omega/k_{2\omega})$, owing to the limitation of the longitudinal phase-matching condition where there is no longitudinal modulation.

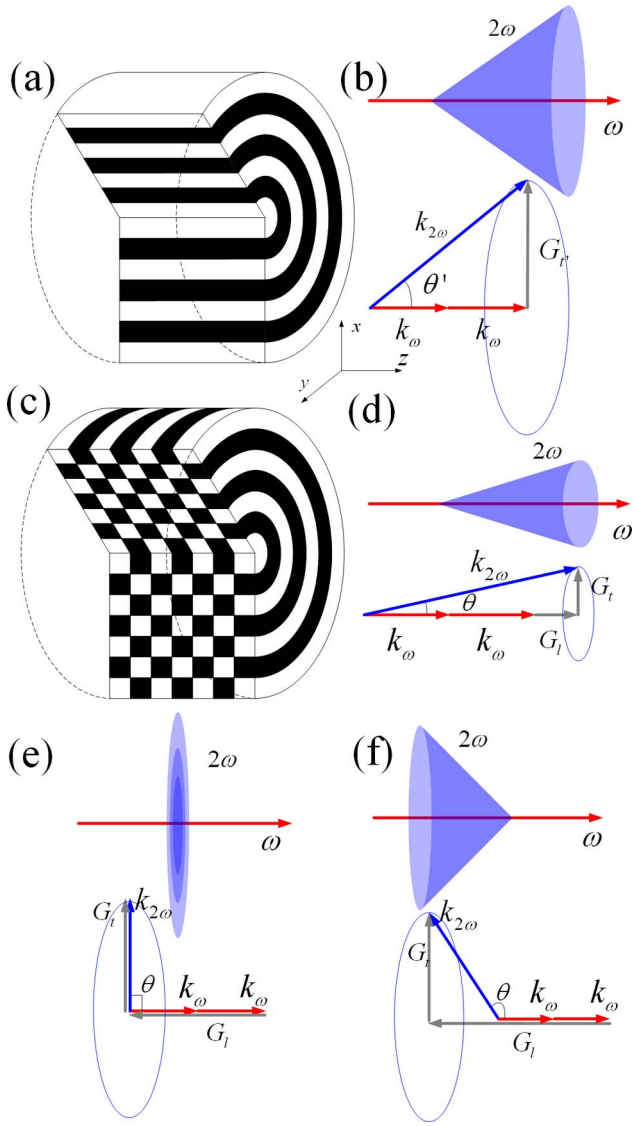

Fig. 1. (Color online) (a) The 2D annular NPC which can only provide (b) the transverse RLV $\vec{G}_t$ and consequently generate the conical harmonic with fixed vertex angle, in contrast to (c) the 3D cylindrical NPC that may offer (d) not only the transverse RLV $\vec{G}_t$ but also the longitudinal RLV $\vec{G}_l$ and therefore produce the conical harmonic with arbitrary angle, for example, (e) the toroid and (f) the counterpropagating cone.

Such an obstacle can be eliminated by extending the annular NPC to the cylindrical structure by adding an additional modulation in the longitudinal direction as shown in Fig. 1(c). Then the phase-matching condition becomes

$$2\vec{k}_\omega + \vec{G}_t + \vec{G}_l = \vec{k}_{2\omega}, \tag{1}$$

so that the extra RLV $\vec{G}_l$ can be offered to help compensate the longitudinal mismatched phase [see Fig. 1(d)]. Thus, the vertex angel 2θ becomes arbitrary through intentionally choosing the proper longitudinal and transverse RLVs, and then many interesting phenomena will be observed. For instance, if θ is set at 90°, the toroidal second harmonic, the so-called T wave [17], will be produced in the cylindrical NPC. Different from the two counterpropagating fundamental beams utilized in [17], the single fundamental beam is used so that the relatively higher conversion efficiency may be obtained for avoiding the spatiotemporal walk-off. In an even more limiting case, if θ is chosen in the range from 90° to 180°, the second harmonic will propagate as a cone along the opposite direction to the fundamental wave.

Figure 2 shows the poling periods of the cylindrical NPC relevant to the transverse and longitudinal phase-matching which are calculated according to the harmonic propagating directions. As we know, the different refractive indices between ordinary and extraordinary harmonics result in different phase mismatches and further lead to the different phase-matching periods. For the ordinary harmonic, because of the refraction being independent of the wave orientation, the transverse and longitudinal periods can be expressed as follows:

$$\Lambda_t^{(o)} = \frac{\lambda}{2n_{o,2\omega}\sin\theta}, \tag{2}$$

$$\Lambda_l^{(o)} = \frac{\lambda}{2|n_{o,2\omega}\cos\theta - n_{o,\omega}|}, \tag{3}$$

where λ is the fundamental wavelength, θ refers to the diffraction angle which is half of the vertex angle of the cone, and $n_{o,\omega}$ and $n_{o,2\omega}$ denote the ordinary principal refractive indices for the fundamental wave and the harmonic, respectively. As for the extraordinary harmonic, since the refraction depends on the wave propagating direction, the transverse and longitudinal periods have the following relation:

$$\Lambda_t^{(e)} = \frac{\lambda}{2n_{2\omega}^{(e)}(\theta)\sin\theta}, \tag{4}$$

$$\Lambda_l^{(e)} = \frac{\lambda}{2|n_{2\omega}^{(e)}(\theta)\cos\theta - n_{o,\omega}|}, \tag{5}$$

with

$$n_{2\omega}^{(e)}(\theta) = \frac{n_{e,2\omega}n_{o,2\omega}}{\sqrt{n_{o,2\omega}^2\sin^2\theta + n_{e,2\omega}^2\cos^2\theta}}, \tag{6}$$

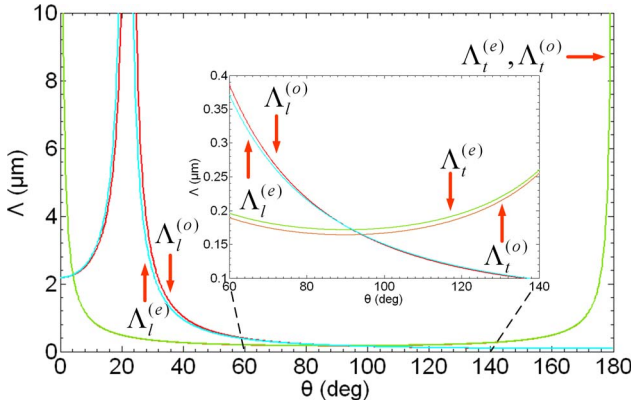

Fig. 2. (Color online) Dependencies of the transverse and the longitudinal phase-matching periods (Λ with subscripts t and l, respectively) for the ordinary and extraordinary harmonic [Λ with superscripts (o) and (e), respectively] on the diffraction angle θ. For convenience of watching, the inset is extracted from the middle section of the curves that are almost coincident.

where $n_{2\omega}^{(e)}(\theta)$ is the extraordinary refractive index varying with the harmonic orientation, and $n_{e,2\omega}$ represents the extraordinary principal refractive index for the harmonic wave.

As illustrated in Fig. 2, by use of the data reported in [25], the calculation is applied to $LiNbO_3$. It can be seen that the curves of the phase-matching periods for the ordinary and extraordinary harmonics are almost coincident in the $LiNbO_3$ crystal. Then the curves will overlap more closely in the $LiTaO_3$ case for the smaller birefringence. Therefore, these two harmonics may together come out of the crystal. In addition, for compensating large phase mismatches, the periods of the first-order QPM are very short with the minimum value down to about 0.1 μm, which is far beyond the state-of-the-art poling technique. The solution is to use the higher-order RLVs just like the thirteenth order used in [14] and, of course, the resulting disadvantage is the inevitable efficiency decrease of the harmonic generation. Nevertheless, in the small θ regime, the RLVs with low order such as first, second, and third order may be utilized due to the transverse periods sharply increasing with the longitudinal ones tending to a stable value of 2.2 μm that can possibly be realized for first-order QPM in experiment. Note that the low-order conical harmonics are also observed in [14], but their mechanism is the nonlinear Raman-Nath diffraction [26] with low second harmonic generation (SHG) efficiency in contrast to the nonlinear Bragg diffraction with relatively high SHG efficiency discussed in this paper. For Raman-Nath diffraction, the longitudinal modulation will not change the diffraction angle because it only needs to satisfy the transverse phase-matching condition. Moreover, on the condition that θ is set at 0° or 22°, the cylindrical NPC will degrade to the 1D periodic or the 2D annular one, because of the transverse or the longitudinal period having a tendency to be infinite.

In analogy to the 1D regime [27], the cylindrical NPC with periodic modulation can be developed to the aperiodic case as shown in Fig. 3(a). The scheme is almost the same, just considering the transverse and the longitudinal modulations as two 1D structures. Then, similarly, the multiple RLVs are obtained in the discrete form in both directions [see Fig. 3(c)] and the multiple conical harmonics with different vertex angles may result from the aperiodic cylindrical NPC as depicted in Fig. 3(b). The generated harmonics may simultaneously exhibit the exceedingly different profiles such as the counterpropagating cone, the toroid, and the short-vertex-angle cone which are discussed above, concentrating on presenting the unique properties of the aperiodic cylindrical NPC. If the azimuthal symmetry of the transverse modulation is changed from continuous to discrete, analogous to the 2D case [28], many new types of cylindrical NPCs may be created to provide RLVs in different spatial distribution.

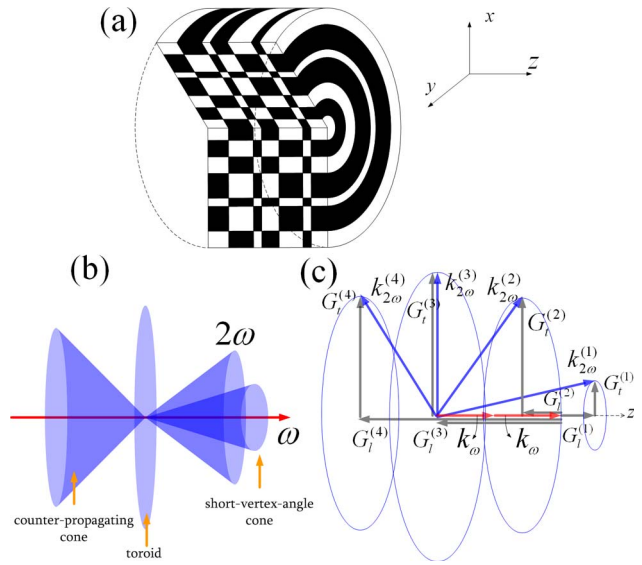

Fig. 3. (Color online) (a) Cylindrical NPC with aperiodic modulation of the quadratic nonlinear coefficient which may supply (c) multiple transverse and longitudinal RLVs in discrete form and then emit (b) the multiple harmonics in different shapes such as counterpropagating cone, toroid, short-vertex-angle cone.

3. EGGLIKE STRUCTURE

It can be seen in the above discussion that either periodic or aperiodic cylindrical NPC may only generate harmonics in one or several directions since only the discrete transverse and longitudinal RLVs can be supplied. Then the question becomes how to emit harmonics in all directions; for example, because the harmonic wavefront is a spherical surface it becomes an interesting problem deserving more studies. Enlightened by the local QPM theory [29], the structure in Fig. 4(a) is designed through programming according to the method suggested in [29], when the focal point of the harmonic which can be considered as the spherical center is set in the crystal. Extending it to the 3D case, the structure that looks like an egg is derived as shown in Fig. 4(b). The RLV distribution of this kind of structure is illustrated in Fig. 4(d), exhibiting a converging tendency. Thus, the spherical harmonic presented in Fig. 4(c) may come out of the egglike structure owing to the phase-matching of SHG in all directions. Note that the crystal should be cut into a ball with the center denoted in Fig. 4(b) so that the generated harmonic wavefront will not be distorted by the surface of the crystal. Consequently, such a 3D NPC can be regarded as a light point source of the harmonic, which cannot be realized in a 1D or 2D structure.

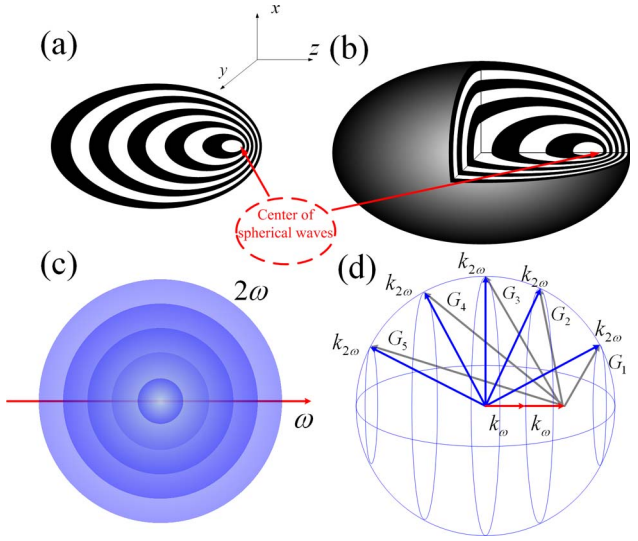

Fig. 4. (Color online) (a) Sectional view of the egglike NPC via programming. (b) Egglike NPC with the denoted center. (c) Generated spherical harmonic. (d) Diagram of the phase-matching condition.

It is obvious that the emission of the harmonic is not isotropic, so the distribution of the intensity on the harmonic wavefront will be studied in the following discussion. As analyzed in [14], the harmonic intensity is proportional to the square of the effective nonlinear coefficient which is relevant to the fundamental and harmonic polarization. $LiTaO_3$ crystal is employed as an example, which is in a trigonal system with a 3 m point group. Since the fundamental beam propagates along the z axis, the ordinary and extraordinary harmonics are azimuthally and radially polarized, respectively, involving the nonlinear components d_{yyy} and d_{zyy}. For convenience of analysis, the walk-off between the harmonic and the fundamental wave is neglected, when the fundamental beam is not tightly focused. So the ordinary and extraordinary harmonic intensities can be given as

$$I_{2\omega}^{(o)} \propto (d_{\mathrm{eff}}^{(o)})^2 = [d_{yyy}\cos(\varphi + 2\gamma)]^2, \tag{7}$$

$$I_{2\omega}^{(e)} \propto (d_{\mathrm{eff}}^{(e)})^2 = [d_{yyy}\cos\theta\sin(\varphi + 2\gamma) + d_{zyy}\sin\theta]^2, \tag{8}$$

where $d_{\mathrm{eff}}^{(o)}$ and $d_{\mathrm{eff}}^{(e)}$ are the effective nonlinear coefficients for the ordinary and extraordinary harmonics, γ is the angle between the fundamental polarization direction and the y axis, φ

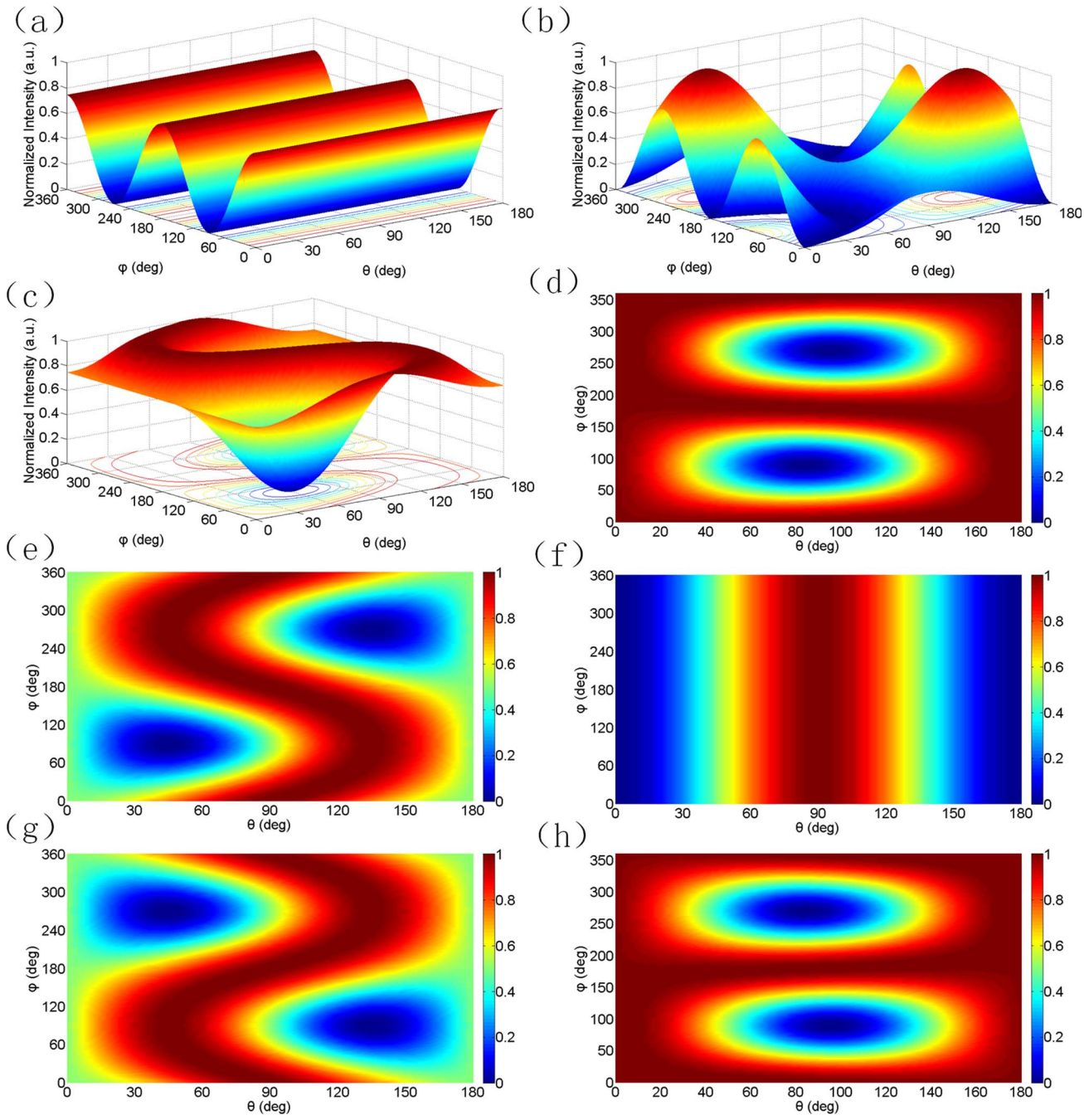

Fig. 5. (Color online) Spatial distribution of (a) ordinary, (b) extraordinary, and (c) total second harmonic intensity in $LiTaO_3$ with $r_d = -1.7$. Corresponding distribution of total second harmonic intensity with variable r_d values, (d) −10, (e) −1, (f) 0, (g) 1, and (h) 10.

is the azimuthal angle of the harmonic with respect to the x axis, and θ is the diffraction angle as defined above.

In theory, a designed egglike NPC can only provide one set of RLVs to enhance one of the ordinary and extraordinary harmonics and suppress the other because of the different phase mismatches. However, as we discussed above, the ordinary and extraordinary harmonics may together come out of the $LiTaO_3$ crystal for short birefringence. Then the total intensity should be a summation in the form $I_{2\omega}^{(\text{total})} = I_{2\omega}^{(o)} + I_{2\omega}^{(e)}$. Suppose $r_d = d_{yyy}/d_{zyy}$ and substitute Eqs. (7) and (8) into the above formula. The total intensity can be expressed as follows:

$$I_{2\omega}^{(\text{total})} \propto [r_d \cos(\varphi + 2\gamma)]^2 + [r_d \cos\theta \sin(\varphi + 2\gamma) + \sin\theta]^2. \tag{9}$$

Consequently, the total intensity of the harmonics is independent of the nonlinear components d_{yyy} and d_{zyy} but dependent on their ratio.

The simulations are performed for $LiTaO_3$ as shown in Figs. 5(a)–5(c) which correspond to $I_{2\omega}^{(o)}$, $I_{2\omega}^{(e)}$, and $I_{2\omega}^{(\text{total})}$, respectively. Like the supposition in [14], γ is set at 0° and r is determined to be −1.7. It is shown that $I_{2\omega}^{(o)}$ only changes with φ while $I_{2\omega}^{(e)}$ varies with both θ and φ. Furthermore, there are two circled cold areas (low intensity areas) in the $I_{2\omega}^{(\text{total})}$ distribution. It is found that the locations of these two cold areas move with the variation of r_d as illustrated in Figs. 5(d)–5(h). For convenience of discussion, the harmonic sphere is viewed as the Earth where $\theta = 0°$ stands for the Arctic, $\theta = 180°$ refers to the Antarctic, and $\theta = 90°$ denotes the equator. At the very beginning, the cold areas lie at the equator with r_d tending to the negative infinity [$r_d = -10$ in Fig. 5(d)]. Then the cold areas gradually move to the two poles with r_d increasing [$r_d = -1$ in Fig. 5(e)]. Note that $LiTaO_3$ is at this state. Next the cold areas completely lie in the Arctic and the Antarctic, respectively [$r_d = 0$ in Fig. 5(f)]. In this situation, the crystal symmetry changes from 3 m to 4 mm because of $d_{yyy} = 0$. Subsequently, the cold areas go back to the equator little by little with r_d increasing to the positive infinity right along [$r_d = 1$ and $r_d = 10$ in Figs. 5(g) and 5(h), respectively]. The $r_d < 0$ and $r_d > 0$ processes are mirror symmetric.

Note that, during the above analysis, there may be an additional azimuthal modulation of harmonic intensities with several peaks due to the artifacts of the discrete character of domain boundaries in ferroelectric crystals [14]. Besides, the difference of the phase-matching conditions for ordinary and extraordinary harmonics is ignored for the crystal with a small birefringence discussed here, while it should be taken into account for the crystal with a large one. Then, conversely, the change of the appearance of $I_{2\omega}^{(\text{total})}$ distribution can be utilized to investigate the large birefringence of the crystal. What is more, only the crystal with 3 m symmetry is studied in this paper while the appearance of $I_{2\omega}^{(\text{total})}$ distribution may change as do the crystals with other symmetries. So the $I_{2\omega}^{(\text{total})}$ distribution can also be used to investigate the crystal symmetry. Studies of other possible applications of the egglike NPC are underway.

4. CONCLUSION

We have proposed, to our knowledge, two novel radially symmetric 3D NPCs: one with a cylindrical structure and one with an egglike structure. The advantage of the periodic and aperiodic cylindrical NPC is that the multiple conical harmonics with arbitrary vertex angels may be produced since the extra longitudinal RLVs can be provided. The dependencies of the phase-matching periods on the diffraction angles are calculated and analyzed. The egglike structure is designed by programming according to the local QPM theory, showing its ability to generate the spherical harmonic as a point light source. The intensity distribution on the harmonic sphere is studied, reflecting a lot of information such as ratio of nonlinear components, crystal symmetry, birefringence, and character of domain boundaries.

ACKNOWLEDGMENTS

This research was supported by the National Basic Research Program "973" of China (2006CB806000), and the Shanghai Leading Academic Discipline Project (B201).

REFERENCES

1. J. A. Armstrong, N. Bloembergen, J. Ducuing, and P. S. Pershan, "Interactions between light waves in a nonlinear dielectric," Phys. Rev. **127**, 1918–1939 (1962).
2. V. Berger, "Nonlinear photonic crystals," Phys. Rev. Lett. **81**, 4136–4139 (1998).
3. S. M. Saltiel, Y. Sheng, N. Voloch-Bloch, D. N. Neshev, W. Krolikowski, A. Arie, K. Koynov, and Y. S. Kivshar, "Cerenkov-type second-harmonic generation in two-dimensional nonlinear photonic structures," IEEE J. Quantum Electron. **45**, 1465–1472 (2009).
4. Y. Sheng, S. M. Saltiel, W. Krolikowski, A. Arie, K. Koynov, and Y. S. Kivshar, "Cerenkov-type second-harmonic generation with fundamental beams of different polarizations," Opt. Lett. **35**, 1317–1319 (2010).
5. Y. Zhang, Z. D. Gao, Z. Qi, S. N. Zhu, and N. B. Ming, "Nonlinear Cerenkov radiation in nonlinear photonic crystal waveguides," Phys. Rev. Lett. **100**, 163904 (2008).
6. Y. Zhang, Z. Qi, W. Wang, and S. N. Zhu, "Quasi-phase-matched Cerenkov second-harmonic generation in a hexagonally poled $LiTaO_3$ waveguide," Appl. Phys. Lett. **89**, 171113 (2006).
7. R. Fischer, S. M. Saltiel, D. N. Neshev, W. Krolikowski, and Y. S. Kivshar, "Broadband femtosecond frequency doubling in random media," Appl. Phys. Lett. **89**, 191105 (2006).
8. A. R. Tunyagi, M. Ulex, and K. Betzler, "Noncollinear optical frequency doubling in strontium barium niobate," Phys. Rev. Lett. **90**, 243901 (2003).
9. P. Molina, M. D. Ramirez, and L. E. Bausa, "Strontium barium niobate as a multifunctional two-dimensional nonlinear 'Photonic Glass'," Adv. Funct. Mater. **18**, 709–715 (2008).
10. P. Molina, S. Alvarez-Garcia, M. O. Ramirez, J. Garcia-Sole, L. E. Bausa, H. J. Zhang, W. L. Gao, J. Y. Wang, and M. H. Jiang, "Nonlinear prism based on the natural ferroelectric domain structure in calcium barium niobate," Appl. Phys. Lett. **94**, 071111 (2009).
11. A. S. Aleksandrovsky, A. M. Vyunishev, I. E. Shakhura, A. I. Zaitsev, and A. V. Zamkov, "Random quasi-phase-matching in a nonlinear photonic crystal structure of strontium tetraborate," Phys. Rev. A **78**, 031802 (2008).
12. M. Baudrier-Raybaut, R. Haidar, P. Kupecek, P. Lemasson, and E. Rosencher, "Random quasi-phase-matching in bulk polycrystalline isotropic nonlinear materials," Nature (London) **432**, 374–376 (2004).
13. Y. Sheng, J. H. Dou, B. Q. Ma, B. Y. Cheng, and D. Z. Zhang, "Broadband efficient second harmonic generation in media with a short-range order," Appl. Phys. Lett. **91**, 011101 (2007).
14. S. M. Saltiel, D. N. Neshev, R. Fischer, W. Krolikowski, A. Arie, and Y. S. Kivshar, "Generation of second-harmonic conical waves via nonlinear Bragg diffraction," Phys. Rev. Lett. **100**, 103902 (2008).
15. S. Saltiel, W. Krolikowski, D. Neshev, and Y. S. Kivshar, "Generation of Bessel beams by parametric frequency doubling in

annular nonlinear periodic structures," Opt. Express **15**, 4132–4138 (2007).
16. S. M. Saltiel, D. N. Neshev, W. Krolikowski, N. Voloch-Bloch, A. Arie, O. Bang, and Y. S. Kivshar, "Nonlinear diffraction from a virtual beam," Phys. Rev. Lett. **104**, 083902 (2010).
17. S. M. Saltiel, D. N. Neshev, R. Fischer, W. Krolikowski, A. Arie, and Y. S. Kivsharl, "Spatiotemporal toroidal waves from the transverse second-harmonic generation," Opt. Lett. **33**, 527–529 (2008).
18. D. Kasimov, A. Arie, E. Winebrand, G. Rosenman, A. Bruner, P. Shaier, and D. Eger, "Annular symmetry nonlinear frequency converters," Opt. Express **14**, 9371–9376 (2006).
19. J. J. Chen and X. F. Chen, "Phase matching in three-dimensional nonlinear photonic crystals," Phys. Rev. A **80**, 013801 (2009).
20. I. T. Wellington, C. E. Valdivia, T. J. Sono, C. L. Sones, S. Mailis, and R. W. Eason, "Ordered nano-scale domains in lithium niobate single crystals via phase-mask assisted all-optical poling," Appl. Surf. Sci. **253**, 4215–4219 (2007).
21. C. E. Valdivia, C. L. Sones, J. G. Scott, S. Mailis, R. W. Eason, D. A. Scrymgeour, V. Gopalan, T. Jungk, E. Soergel, and I. Clark, "Nanoscale surface domain formation on the $+z$ face of lithium niobate by pulsed ultraviolet laser illumination," Appl. Phys. Lett. **86**, 022906 (2005).
22. S. Fahy and R. Merlin, "Reversal of ferroelectric domains by ultrashort optical pulses," Phys. Rev. Lett. **73**, 1122–1125 (1994).
23. H. S. Zhu, X. F. Chen, H. Y. Chen, and X. W. Deng, "Formation of domain reversal by direct irradiation with femtosecond laser in lithium niobate," Chin. Opt. Lett. **7**, 169–172 (2009).
24. H. Lao, H. Zhu, and X. Chen, "Surface ablation of congruent and Mg-doped lithium niobate by femtosecond laser," Laser Phys. **20**, 245–249 (2009).
25. G. J. Edwards and M. Lawrence, "A temperature-dependent dispersion-equation for congruently grown lithium-niobate," Opt. Quantum Electron. **16**, 373–375 (1984).
26. S. M. Saltiel, D. N. Neshev, W. Krolikowski, A. Arie, O. Bang, and Y. S. Kivshar, "Multiorder nonlinear diffraction in frequency doubling processes," Opt. Lett. **34**, 848–850 (2009).
27. B. Y. Gu, B. Z. Dong, Y. Zhang, and G. Z. Yang, "Enhanced harmonic generation in aperiodic optical superlattices," Appl. Phys. Lett. **75**, 2175–2177 (1999).
28. N. Voloch, T. Ellenbogen, and A. Arie, "Radially symmetric nonlinear photonic crystals," J. Opt. Soc. Am. B **26**, 42–49 (2008).
29. Y. Q. Qin, C. Zhang, Y. Y. Zhu, X. P. Hu, and G. Zhao, "Wave-front engineering by huygens-fresnel principle for nonlinear optical interactions in domain engineered structures," Phys. Rev. Lett. **100**, 063902 (2008).